A multiphase variational level set approach for modelling human embryos

Uffe Damgaard Pedersen and Ole Fogh Olsen
The IT University of Copenhagen
Glentevej 67, DK-2400 Copenhagen, Denmark
email: udp@itu.dk, fogh@itu.dk

Niels Holm Olsen
Department of Computer Science, University of Copenhagen
Universitetsparken 1, Copenhagen , Denmark
email: qwer@diku.dk

Abstract

We propose to model the 3d shape and relative position of blastomeres confined inside the zona pellucida in human embryos with a multiphase variational level set approach.

The blastomeres and the volume bounded by the interior surface of the zona pellucida are modelled as elastical objects with different surface tension. The object positions are constrained by measurements from light microscopy images and a non-overlapping criterium. Each object surface must contain a specified curve and the location of the entire object surface is restricted to the closure of the interior of a generalized cylinder given by the same curve. The general approach has been extended with a method representing these as soft constraints. There is no quantitative golden standard to measure the results against so the evaluation is based on judgement from human experts. The method results in models which corresponds well with human expert interpretation of the light microscopy images. This deformable model can capture the important deformations caused by mutual interaction between the blastomeres in contrast to previous models.

1. Introduction

Fertility clinics need to assess the quality of human embryos to ensure high chance of pregnacy and at the same time avoid multiple siblings. The present state of the art is to select the best candidate embryos by visual inspection of microscopy images by medical experts. Medical experts believe in an increase in overall quality by moving from qualitative to quantitative inspection and from 2D to 3D.

The morphology of the human embryos can be probed using Hoffman modulation contrast light microscopy images[2, 3, 1]. This image modality fulfills the obvious and crucial requirement of a non-invasive image acquisition technique. We introduce the embryo morphology and the Hoffman modulation contrast technique in section 2.

The complexity of the image modality allows only the contour locations of the object to be quantitatively measured from an embryo with blastomeres. Section 3 will describe this step of intermediate processing for extracting the trustworthy information from the images.

The extracted information provides us with some geometrical constraints on the surfaces of the objects of interest. The prior expectations of the behavior of the biological objects from medical experts allow us to formulate energies for minimisation such that the prior and the data select a configuration of the surfaces of the biological objects. In section 4 we present how to model these objects with multiple non overlaping level sets with minimal surface tension and constant volume. The approach is inspired by a method proposed for studying the behavior of bubbles and drops by Zhao et al. [5, 6].

The section 5 and 6 respectively present the results in terms of surface renderings and evaluation by experts and conclude on the achieved results.

2 Morphology and Light Microscopy

Figure 1 illustrates a morphology model of a human embryo that the biologists use.

Though the models are drawn in 2D, the biologists think of them as 3D objects and are interested in 3D embryo morphology measures like the volumes and surface areas of the different subparts. At day 2, after the fertilization, they are interested in the number of and sizes and shapes of the divided cells (blastomers), and their geometrical orientation relatively to each other.

In this article we use the term Zona Pellucida for describing the inner surface of the Zona Pellucida.

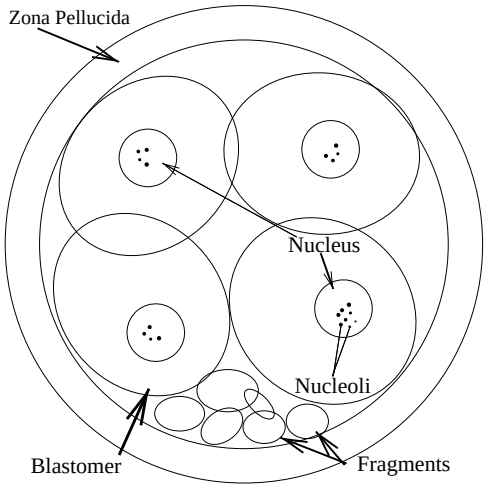

Figure 1. Morphology model of embryo at day 2 after fertilization.

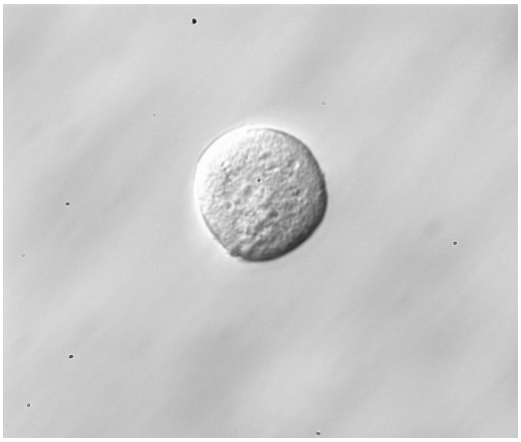

Figure 2. HMC image of an isolated human blastomere.

2.1 Hoffman Modulation Contrast Light Microscopy

By focusing the microscope at different optical sections, the three-dimensional structure of the embryo may be studied. However, quantitative 3D volumetric reconstruction is a difficult inverse problem due to the complicated image formation.

The image formation is a result of both the optical characteristics of the embryo and the microscope optics used. Human embryos are microscopically "large", transparent but refractive objects, so the usual model of rectilinear light propagation does not hold. Refractive objects are also known as phase objects, since they interact with the light by changing its phase and thus causing different delays and ray deflections. Their transparent property calls for the use of a contrast technique.

Hoffman Modulation Contrast (described first in [2, 3, 1]) is a light microscopy contrast technique, well suited for in vivo studies of biological specimen, because of its non-invasive contrast generation for transparent but refracting objects[1]. Figure 2 shows an example HMC image of an isolated blastomere and Figure 5 shows an example of four blastomeres in a human embryo.

The HMC technique generates contrast by converting "phase gradients" or "optical gradients" into intensity variations in the microscopy images[2] such that positive gradients show up bright and negative gradients show up dark. This results in images that give a human observer the familiar but in this situation false impression[2] of looking at the highlights and shadows resulting from a surface with height variations, shined upon from one side. Fortunately for the human observer, this misinterpretation, somewhat compensates for the assymmetric artificially generated contrast in the HMC images, and results in a geometrical impression qualitatively similar to the object geometry.

Figure 3 illustrates the principle of the HMC technique. As described in [2] and [3], the HMC technique uses a rectangular slit illuminating aperture placed in the front focal plane of the condenser of the microscope, together with an aligned amplitude modulating filter with a dark, a grey and a bright region placed in the conjugate back-focal plane of the objective lens. The setup achieves that rays deflected in one direction are atenuated while those deflected in the opposite direction reach the image plane unaffected.

The HMC technique is especially well suited for studying anomalous diffractive objects such as blastomeres (the major subparts of the human embryo). When focusing on a blastomere, this technique most clearly reveals the blastomere contours as image intensity ridges and valleys, while the central parts are imaged using intermediate intensities reflecting the local optical gradient of the phase object.

3 Extracting information from HMC images

From HMC images of isolated blastomeres outside the human embryo a quantitative reconstruction of the optical thickness profile can be found and with that a 2D surface model. However when studying multiple blastomeres in a single embryo this route of reconstruction is not straight forward due to the non-trivial (non-linear) interaction between the different blastomere images, and the lack of a single in-focus image. Because of this it is only the contour locations which can be quantitatively measured from an embryo with blastomers. Hence information is solely extracted from the HMC images by detecting the large outline of the cells (the blastomeres) and the egg shell (zona pellucida).

3.1 Extracting 2D contours

In theory the HMC technique generates maximum image contrast where the light touches the blastomere surface

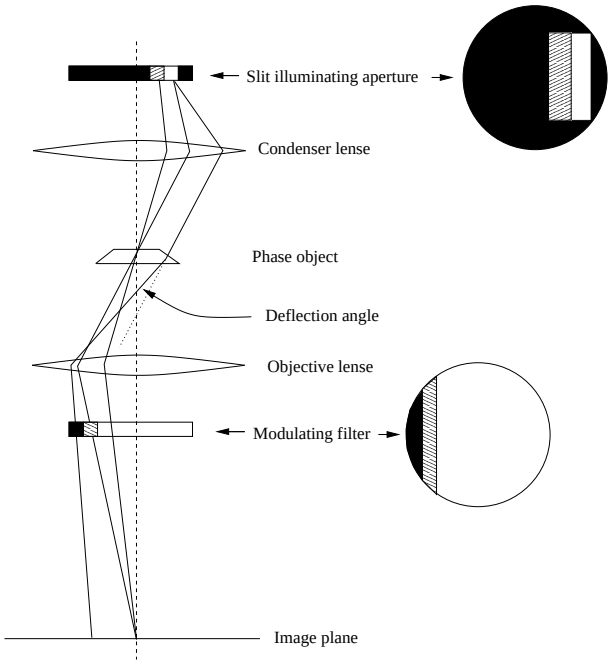

Figure 3. The HMC microscope model [1].

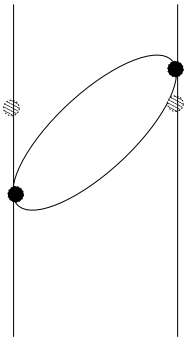

Figure 4. Equator contours. The blastomere contour (here marked by black dots in a 2D orthogonal projection) is annotated manually (here marked by grey dots) in the image where the blastomere is judged to be most in focus.

tangentially and the largest deflection angles are realized. This curve embedded in 3D does in general not lie in a single plane perpendicular to the optical axis. However, do to the lack of resolution in the direction of the optical axis the curve is approximately described in one single plane where the blastomere is seen to be most in focus (see Figure 4). For each of the blastomeres the rim contour will thus be restricted to lie entirely in one of the images in the focus sequence, judged to be the "equator image" of the blastomere. Hence the blastomere equator contour curve is represented by a curve in a 2D plane together with the z-position of the equator image. An example for an embryo with four blastomeres is in figure 5. The extracted curves are superimposed on the corresponding infocus HMC images.

Due to the acquisition method the contour is interpreted as the shadow outline of the object. One can deduce that the surface of the object is lying within the generalized cylinder sweped by the extracted curve and that the curve must be part of the surface. These two conditions are geometrical constraints known for each blastomere and for zona pellucida.

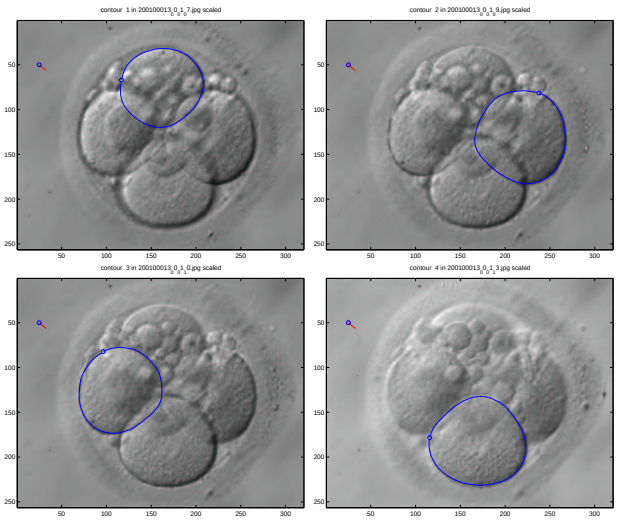

Figure 5. Embryo 13. The 2D equator contours of blastomeres is evident from HMC light microscopy images of human embryos. The four images have been selected from a focus-sequence as the equator planes of each of the 4 blastomeres, and the 2D contour of the infocus blastomere has been identified. The z-position of the equator contour is known from the focus position of each image in the sequence.

4 Modeling Blastomeres and Zona Pellucida

The zona pellucida and each of the blastomeres are modelled using a level set function $\phi_i, i = 1, \ldots, n$. The extend and position of the blastomere (and zona pellucida) from the measurements are bounded by two fixed level sets. The allowed region for a blastomere is bounded by the fixed level set function denoted $\psi_i, i = 1, \ldots, n$. In one vertical plane the blastomere is confined to a specific

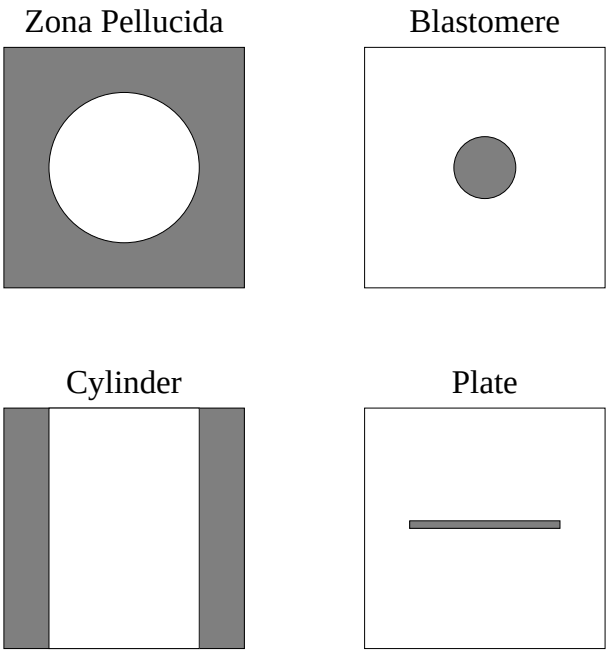

Figure 6. Here is illustrated the sign convention of the different level set functions. Grey denotes positive sign and white denotes negative.

curve, the level set function χ_i controls this together with ψ_i.

Under the constraint of volume preservation we minimise the tension of the surfaces and the overlap between the relevant level sets. Overlap is measured as the intersection of the positive parts of the corresponding level set functions. Figure 6 illustrates the sign convention of the level set functions. We want non overlap between the level set functions for all blastomeres and for the zona pellucida; non overlap between a blastomere and its related generalized cylinder ψ_i; non overlap between the complement of the zona pellucida and its related cylinder. Finally to ensure that the given contour is part of the blastomere a "flat" plate-like level set function χ_i must be completely overlapped by its associated blastomere. Because of the sign convention for zona pellucida it is not allowed to overlap its associated plate.

The central idea is illustrated in 2D in figure 7. In the initial state there is a slight and not allowed overlap between blastomeres. As the energies are minimized in time under the constraint, the blastomeres fit within the zona pellucida and adjust their shape to each other and at the same time remain within the specified positions.

4.1 Review of the variational level set formulation

We follow Zhao et al. [5, 6] in their formulation of the general variational level set formulation of multiphase problems. Minimize

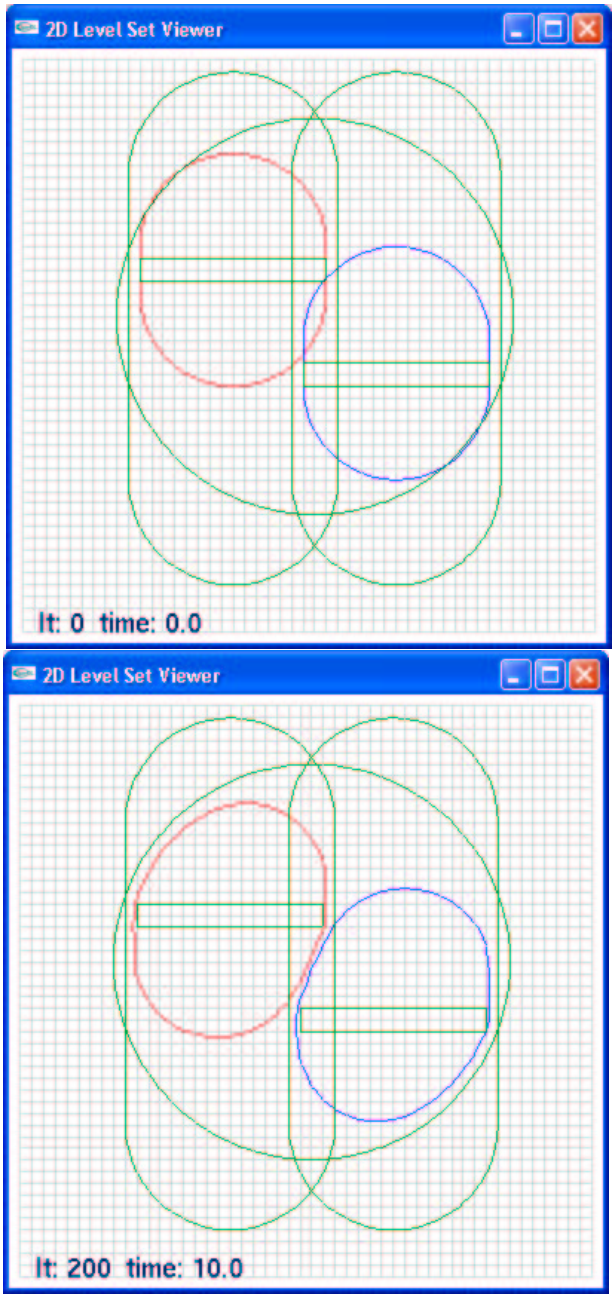

Figure 7. Illustration from a 2D implementation of the method. There are five closed curves and two horisontal plates (bars) in each subfigure. The large circle represents zona pellucida. The two closed curves surrounding the smallest areas represents two blastomeres. From the top subfigure with the initial configuration these two evolve to the bottom subfigure. The rest remains fixed in position. The last two closed curves and the two plates are the geometric bounds on the blastomeres. Each of the two closed curves restricts the corresponding blastomere, which has to stay inside. The two fixed plates have to stay inside the corresponding blastomere and represent the user defined curve. The plate and cylinder representing the bounds on zona pellucida are not shown.

$$E = \int F(f_1(\bar{x}), f_2(\bar{x}), \ldots, f_n(\bar{x}))d\bar{x}$$

subject to the constraints

$$\int g_j(f_1(\bar{x}), f_2(\bar{x}), \ldots, f_n(\bar{x}))d\bar{x} = C_j, \quad j = 1, \ldots, m$$

Using Rosen's gradient project method [4] , we get the following coupled system of partial differential equations:

$$\frac{\partial f_i}{\partial t} = -\frac{\partial F}{\partial f_i} - \sum_{j=1}^{m} \lambda_j \frac{\partial g_j}{\partial f_i} \tag{1}$$

where λ_j is a Lagrange multiplier. The constraints fulfill

$$\frac{d}{dt} \int g_j(f_1, f_2, \ldots, f_n)d\bar{x} = 0, j = 1, \ldots, m$$

which determines the Lagrange multipliers as solutions of the linear system:

$$\begin{aligned} \sum_{k=1}^{m} \lambda_k \int (\nabla_f g_j \cdot \nabla_f g_k)d\bar{x} &= -\int (\nabla_f g_j \cdot \nabla_f f)d\bar{x} \\ \text{where } j = 1, \ldots, m \text{ for } f &= (f_1, \ldots, f_n) \end{aligned} \tag{2}$$

In order to measure overlap we simply compare the output of the Heaviside function applied to the level sets.

$$H(x) = \begin{cases} 1, & x \geq 0 \\ 0, & x < 0 \end{cases}$$

We will also need the distributional derivative of the Heaviside function which is the Dirac delta function $\delta(x)$.

4.2 Model energies and constraints

We have the following energies and constraints in play. The surface tension energy for one level set :

$$E_{surf} = \int \gamma_i \delta(\phi_i(\bar{x}))|\nabla \phi_i(\bar{x})|d\bar{x} \tag{3}$$

where γ_i is surface tension coefficient for surface i. This models the elasticity. Next is the constraint of volume preservation:

$$\int H(\phi_i(\bar{x}))d\bar{x} = V_i \tag{4}$$

where V_i is the constant enclosed volume for respectively the blastomeres and the zona pellucida.

The next energy expresses the overlap between an active level set function and the rest of the active level set functions (blastomeres and zona pellucida):

$$E_{overlap} = \int H(\phi_i(\bar{x})) \left(\left[\sum_{j=1}^{n} H(\phi_j(\bar{x})) \right] - H(\phi_i(\bar{x})) \right) d\bar{x} \tag{5}$$

The overlap between a blastomere (or zona pellucida) and its bounding cylinder:

$$E_{cyl} = \int H(\phi_i(\bar{x}))H(\psi_i(\bar{x}))d\bar{x} \tag{6}$$

The overlap between the complement of the blastomere (or zona pellucida) and its restricting plate.

$$E_{plate} = \int H(-\phi_i(\bar{x}))H(\chi_i(\bar{x}))d\bar{x} \tag{7}$$

The level set ϕ_1 represents the zona pellucida and has a special sign convention (please see figure 6). Consequently in the above equations 4, 6 and 7 the sign in front of ϕ_1 should be flipped.

4.3 Minimization

All overlap and the surface tension are to be minimized under the constraint of volume preservation. The resulting energy functional to be minimized is then:

$$E = E_{surf} + E_{overlap} + E_{cyl} + E_{plate}$$

under the constraint specified in the equation 4

Using Rosen's gradient projection method we obtain the system evolution equations, a coupled set of partial differential equations, for the blastomeres and zona pellucida level set functions:

$$\begin{aligned} \frac{\partial \phi_i}{\partial t} &= |\nabla \phi_i(\bar{x})| \left(\gamma_i \nabla \cdot \left(\frac{\nabla \phi_i(\bar{x})}{|\nabla \phi_i(\bar{x})|} \right) \right. && (8) \\ &- \left[\sum_{j=0}^{n} H(\phi_j(\bar{x})) - H(\phi_i(\bar{x})) \right] && (9) \\ &- H(\psi_i(\bar{x})) && (10) \\ &+ H(\chi_i(\bar{x})) && (11) \\ &- \lambda_i) && (12) \end{aligned}$$

The corresponding Lagrange multiplier:

$$\begin{aligned} \lambda_i &= \int_\Omega \delta(\phi_i(\bar{x}))|\nabla \phi_i(\bar{x})| \left(\gamma_i \nabla \cdot \left(\frac{\nabla \phi_i(\bar{x})}{|\nabla \phi_i(\bar{x})|} \right) \right. && (13) \\ &- \left[\sum_{j=0}^{n} H(\phi_j(\bar{x})) - H(\phi_i(\bar{x})) \right] && (14) \\ &- H(\psi_i(\bar{x})) && (15) \\ &+ H(\chi_i(\bar{x})))d\bar{x} && (16) \\ &/ \int_\Omega \delta(\phi_i(\bar{x}))|\nabla \phi_i(\bar{x})|d\bar{x} && (17) \end{aligned}$$

Please note that in the equations 8 through 17 the common factor $\delta(\phi_i(\bar{x})$ has been replaced by a $|\nabla \phi_i(\bar{x})|$. This time rescaling does not effect the solution only the speed of descent (see [5] for more details)

As a consequence of the sign changes for the energy terms for zona pellucida ϕ_1, the signs in the following equations 10, 11,15 and 16 are flipped for $i = 1$

The extension to the approach by Zhao et al. [5, 6] is that we have formulated the geometrical constraints on the position and extend of the objects using level sets.

We use the simple forward Euler discretisation in the time direction. The term $|\nabla\phi_i(\bar{x})|$ is calculated with a first order upwind scheme based on the sign of the sum of the equations 14, 15 and 16. The curvature part is discretised by twice applying a central scheme with a step size of one half. More details can be found in Zhao et al. [5]

5 Experiments and Results

The above described method, has been implemented and applied to 4 HMC-image focus sequences of human embryos, with expert annotations of the zona pellucida and blastomere contours. The four presented data sets have been selected out of 20 sets based on the following criteria: the same number of blastomeres, good annotations without errors and being "typical" embryos. Each image sequence consisted of 17 images focused 5 micrometers apart.

From these annotations the bounding cylinder and plate level set functions were automatically created in a 75x75x75 discrete voxel grid. The zona pellucida and blastomere level set functions were initialized as approximating spheres. The centers were placed midway between the extremal contour locations along each of the two image axes and at the vertical position of the in-focus image.

Based on expert expectations of the objects being close to spheres we initialized the individual blastomeres as spheres using a radius given by the average diameter of the contour.

The ratio between the used surfaces tensions was based on expert expectations that the zona pellucida has the highest surface tension. The absolute offset of surface tension gives a weighting between overall surface tension and the energy describing overlap. We have used equal surface tensions of 1 for all blastomeres and a surface tension of 5 for the zona pellucida.

We used a fixed step size of 0.002 in the forward Euler discretization, and ran it for 5000 iterations. We reached an approximately stationary solution after about 3000 iterations.

5.1 Results

In the following presentations of the 3D results we will not illustrate the restricting level sets. The figures will show the level sets which represent the physical objects: zona pellucida and the blastomeres. In some figures the annotated curves are superimposed.

As can be seen by comparing figure 8 and figure 5 the stationary blastomere surface solutions have outlines (seen from above) very similar to but not exactly equal to the annotated contours. This close agreement shows that the soft implementation of the contour constraint by minimization of the two energy functionals described by equations 6 and 7 expressing overlap with the bounding cylinder and plate, works well.

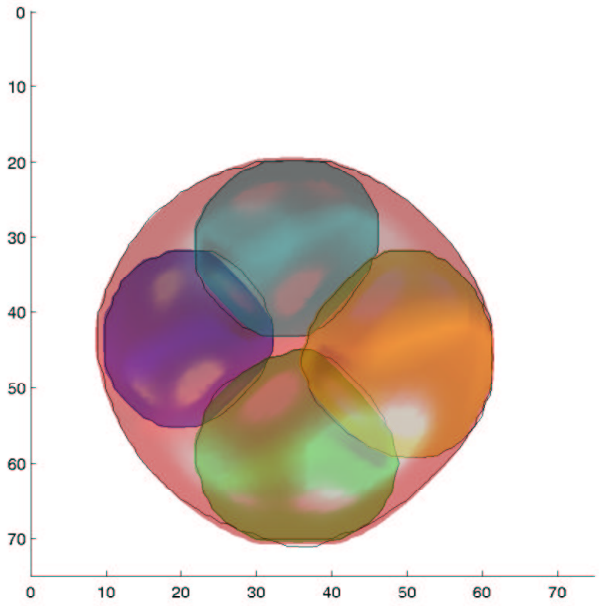

Figure 8. Four blastomeres within the zona pellucida. Embryo number 13. With bounding curves. Compare with images in Figure 5

In figure 9 we see that the blastomeres and the zona pellucida are attached to the given contours (at the desired vertical positions). This verifies that the interplay between the cylinder (equation 6) and the plate (equation 7) works as expected. It is also seen that the bottom left blastomere in this view has an indentation on its top right side, right above its attachment to its contour. We interpret this indentation as a result of another blastomere pressing upon it as a result of the non-overlapping functional. It is thus seen that the simple sphere model which we used for initialization is not possible without overlapping. Since we initialize with spheres we have a bias towards too big volumes. The excessive volume has to be distributed within the cylinder which occasionally give partly cylinder-like shapes (see Figure 10).. This could of course be "fixed" by lowering the initial volume size but such an ad hoc "fix" would not really solve the underlying problem of unknown volume sizes.

Our model supports the fact the blastomeres are not spheres, but deformed due to mutual physical interaction. The figures 11 and 12 illustrates the model of two other Embryos. It has been checked but not illustrated that the overlap between the blastomeres is below the resolution of the model. All overlap extend less than one voxel width into another object. Overlap occurs in connect with (in-

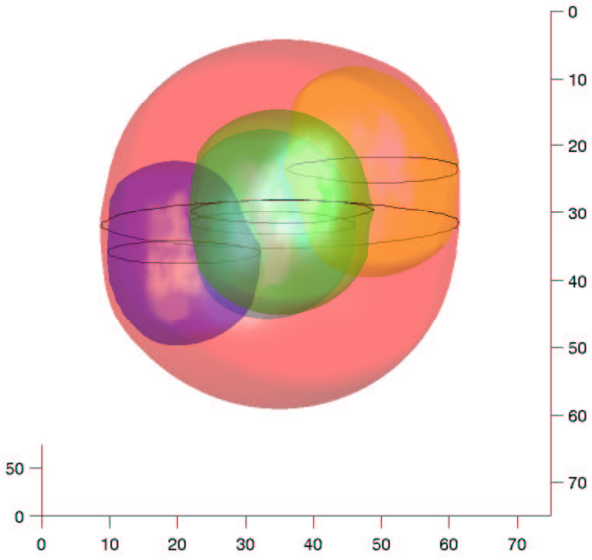

Figure 9. Four blastomeres within the zona pellucida. Embryo number 13

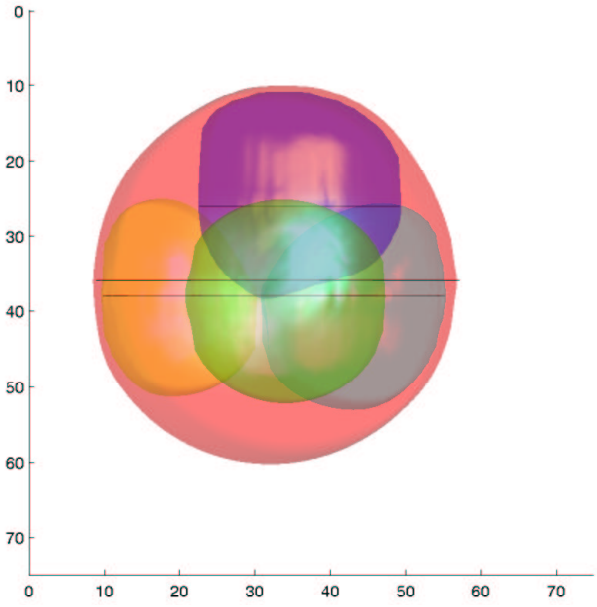

Figure 10. Four blastomeres within the zona pellucida. Embryo number 22

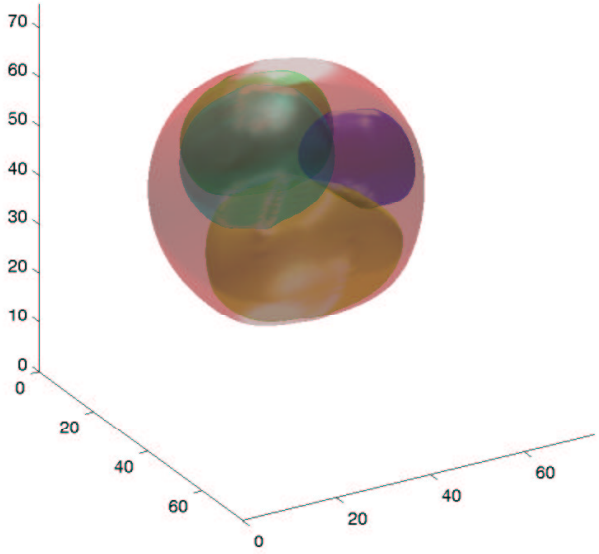

Figure 11. Four blastomeres within the zona pellucida. Embryo number 30

consistent) contour constraints.

Fertility experts have evaluated the model results against their visual interpretation of the original images and concluded that the results are very realistic considering the uncertainty in the direction of the optical axis.

6. Conclusion

We have successfully applied the general multiphase variational level set approach to a new application area of modeling human embryos. The general approach has been extended with a method for representing geometric conditions with level sets. The extension allows a seemless integration of these conditions into the general framework. Medical experts have concluded that these preliminary modeling results of human embryos agree well with the expected behavior of the subparts of a human embryo. The models give a realistic answer to the raised question : what is the 3D shape and configuration of the blastomeres within the zona pellucida.

One of the drawbacks of the presented method is the need to fix the volume of each sub object from the start. A next step would be to optimize the volumes such that the stable state of the objects would have the outline contours as a property in the solution and not as a constraint enforced by the optimization technique. This will be addressed in future work.

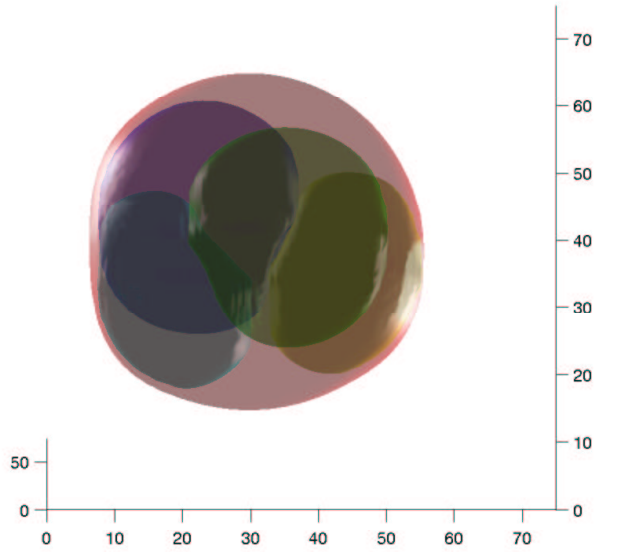

Figure 12. Four blastomeres within the zona pellucida. Embryo number 43

7. Acknowledgement

The authors would like thank Christina Hnida and Sren Ziebe for the acquisition and annotation of the HMC images of human embryos and blastomeres, at the Fertility Clinic, University Hospital of Copenhagen, Denmark. The images were acquired using the FertiGrab system equipped with a multi focus module available from IH-Medical, Image House A/S, Denmark.

References

[1] R. Hoffman. The modulation contrast microscope: principles and performance. *Journal of Microscopy*, 110:205–222, August 1977.

[2] R. Hoffman and L. Gross. The modulation contrast microscope. *Nature*, 254:586–588, Apr. 1975.

[3] R. Hoffman and L. Gross. Modulation contrast microscope. *Applied Optics*, 14(5):1169–1176, May 1975.

[4] G. Rosen. The gradient projection method for nonlinear programming part 2, nonlinear constraints. *J.Soc.Indus.Appl.Math*, 9, 1961.

[5] H.-K. Zhao, T. Chan, B. Merriman, and S. Osher. A variational level set approach to multiphase motion. *Jounral of Computational Physics*, 127:179–195, 1996.

[6] H.-K. Zhao, B. Merriman, S. Osher, and L. Wang. Capturing the behavior of bubbles and drops using the variational level set approach. *Journal of Computational Physics*, 143:495–518, 1998.